# Instability and Flow Localization During Compression of a Flow Softening Material

*M. Thirukkonda, R. Srinivasan, and I. Weiss*

**Materials that flow soften exhibit plastic instability during compressive deformation when Considere's criterion is satisfied, i.e., when there is no increase in the force required to cause deformation. Further, theories developed by Hart and Jonas et al. show that the flow localization can occur during plastic instability. The strains at which the onset and termination of flow localization occur depend on the strain-rate sensitivity of the material. Flow localization initiates earlier and terminates later for a strain-rate sensitive material in comparison to a rate insensitive material. However, in an apparent contradiction, the deformation is more homogeneous in a strain-rate sensitive material.**

**This paper presents the results of an investigation, using computer simulation, to visualize the deformation during constant strain-rate compression of flow softening materials with different strain-rate sensitivity. The effect of strain-rate sensitivity on the initiation and termination of plastic instability and flow localization due to mechanical damage, geometric nonuniformities, and friction were studied. Parameters developed to describe the extent of inhomogeneity during deformation are used to explain the conclusions made by Jonas et al.**

**Keywords**

dead metal zone, finite element method, flow localization, inhomogeneous deformation, plastic instability, slab analyis, shear band, strain rate localization

## 1. Introduction

MANY materials exhibit flow softening behavior at elevated temperature where flow softening is defined as a decrease in the stress required to cause deformation with increasing strain. A number of different mechanisms for flow softening have been proposed. These include dynamic recovery, dynamic recrystallization, geometric nonuniformities, deformation heating, rearrangement of phases, coarsening of precipitates, and phase changes during deformation (Ref 1). During tensile deformation, materials exhibit an instability when the force required to cause deformation does not increase with increasing strain. Considere (Ref 2) showed that for a strain-rate insensitive material, the strain at which instability occurs is related to the rate of work hardening. Further, any local variations in area get amplified with additional deformation, i.e., the deformation localizes. Hart (Ref 3) then showed that for a strain-rate sensitive material, maximum load occurs at the strain when the work hardening parameter $\gamma = (1 + m)$ during constant elongation rate deformation, and when $\gamma = 1$ during constant strain-rate deformation, while deformation localization starts at the strain when $\gamma = (1 - m)$. The work hardening parameter $\gamma$ is defined as:

$$\gamma = \frac{1}{\sigma}\left(\frac{\partial \sigma}{\partial \varepsilon}\right)_{\dot{\varepsilon}, T} \quad \text{(Eq 1)}$$

where $m$, the global strain-rate sensitivity parameter, is assumed to be constant during deformation.

**M. Thirukkonda, R. Srinivasan,** and **I. Weiss,** Mechanical and Materials Engineering Department, Wright State University, Dayton, OH 45435, USA

During tensile deformation of a strain hardening material, $\gamma$ is generally positive and decreases with increasing strain. Therefore, for a material with a high strain-rate sensitivity, the deformation may become unstable at a low value of strain, but localization of deformation may not occur until larger values of strain have been attained (Ref 4).

Compressive deformation of work hardening materials is inherently stable because both the flow stress and area increase as deformation progresses. However, for a flow softening material, if the stress decreases at a rate greater than the rate of increase of area, the deformation may become unstable. That is, deformation occurs without an increase in load, and deformation localization can occur. Jonas, Holt, and Coleman (Ref 4) showed that unstable deformation occurs between two values of strain: when $\gamma = 1$ for constant strain-rate deformation, and when $\gamma = (1 + m)$ for constant ram displacement rate. They define two types of localization: flow localization, which is when the rate of change of area at a region of inhomogeneity exceeds that in the bulk, and strain-rate localization, which is when the strain rate in a region of inhomogeneity exceeds that in the bulk. The first type of localization is the same as defined by Hart and starts when $\gamma = (1 - m)$. Strain-rate localization is similar to that considered by Considere and occurs between strains when $\gamma = 1$. As the strain-rate sensitivity of a material increases, the two values of strain at which $\gamma = (1 - m)$ move farther apart, and flow localization occurs for a longer time. However, Jonas and Luton (Ref 1) also conclude that when flow softening occurs, the amount of inhomogeneous deformation decreases as strain-rate sensitivity increases.

This paper examines this apparent contradiction that increasing strain-rate sensitivity, on the one hand, increases the period of nonhomogeneous deformation, while on the other hand, decreases the amount of nonhomogeneous deformation. We studied the effect of strain-rate sensitivity on the various parameters associated with inhomogeneous deformation by first using a slab analysis technique similar to that of Hart and Jonas et al. (Ref 4, 5) in which strips of material are assumed to deform independent of each other while supporting the same ap-

plied axial load. Then we used finite element simulation to examine the development of inhomogeneous deformation under similar conditions.

In the following sections, we have adopted the convention that compressive stresses, strains, and strain rates are negative. Some of our results are, therefore, plotted in the third quadrant.

## 2. Slab Analysis of Inhomogeneous Deformation During Compression

Consider a cylindrical compression sample to be made of a series of thin disks that deform with no friction at the interfaces between the disks. Then, as shown by Jonas and Baudelet (Ref 5), at any instant of time, $t$, since the same force is supported by each disk,

$$\left(\frac{\partial \ln F}{\partial x}\right)_t = 0 = \left(\frac{\partial \ln A}{\partial x}\right)_t + \left(\frac{\partial \ln \sigma}{\partial x}\right)_t \quad \text{(Eq 2)}$$

where $F$ is the applied axial load, $x$ is the position along the length of the sample, and $A$ is the cross sectional area of the sample. If there are variations in strain or geometrical nonuniformities within the specimen, then (Ref 5):

$$m\left(\frac{\partial \ln \dot{\varepsilon}}{\partial x}\right)_t = \left(\frac{\partial \varepsilon}{\partial x}\right)_t [1-\gamma] - \frac{d \ln A_0}{dx} \quad \text{(Eq 3)}$$

The last term in the above equation is an initial variation in cross sectional area of the specimen. Equation 3 can be used to follow the evolution of inhomogeneous deformation due to either mechanical damage, when a small area is subjected to an initial prestrain, or machining defect, when there is an initial variation in cross sectional area, i.e., $(d \ln A_0/dx) \neq 0$. The effect of stress triaxiality, which would arise due to nonuniform cross-sections, was neglected in this analysis.

### 2.1 *Case 1: Effect of Machining Defect*

When a machining defect is present, the area of one region of the specimen is different from the area of the rest of the specimen. Let the initial area of the bulk be $A_0$ and the inhomogeneity be a bulge of initial area $A_{b0}$. There is no initial difference in strain between the bulge and the bulk of the specimen. It can be shown (Ref 5) that at any instant of time, $t$, the incremental differences in strain rate and rate of change of area in these two regions are:

$$\delta \ln \dot{\varepsilon} = \frac{(\gamma - 1)}{m} \delta \ln A - \frac{1}{m} \delta \ln A_0 \quad \text{(Eq 4)}$$

and

$$\delta \ln \dot{A} = \frac{\gamma - 1 + m}{m} \delta \ln A - \frac{\gamma}{m} \delta \ln A_0 \quad \text{(Eq 5)}$$

In the above equations, the symbol $\delta$ represents the incremental differences in the area or the strain rate between two regions of the specimen, and the subscript 0 indicates initial conditions. These two equations were used to calculate the area and the strain rate in the bulge at any time $t + \Delta t$ as given below:

$$\left(A_b\right)_{t+\Delta t} = \left(A_b\right)_t + \left(A_{t+\Delta t} - A_t\right) \left[\frac{\left(\frac{A_b}{A}\right)^{\beta}}{\left(\frac{A_{b0}}{A_0}\right)^{\frac{\gamma}{m}}}\right]_t \quad \text{(Eq 6)}$$

and

$$\dot{\varepsilon}_b = \dot{\varepsilon} \left[\frac{\left(\frac{A_b}{A}\right)^{\frac{\gamma-1}{m}}}{\left(\frac{A_{b0}}{A_0}\right)^{\frac{1}{m}}}\right] \quad \text{(Eq 7)}$$

where

$$A = A_0 \exp(-\dot{\varepsilon} t) \quad \text{(Eq 8)}$$

and

$$\beta = \frac{\gamma - 1 + m}{m} \quad \text{(Eq 9)}$$

### 2.2 *Case 2: Effect of Mechanical Damage*

In the case of mechanical damage to the specimen, the cross sectional area is assumed to be initially uniform, but a small region has been prestrained to a strain of $\varepsilon_0$. In this case, it was shown that at time, $t$, the differences in strain rate and rate of change of area between the damaged and undamaged regions of the specimen are given by (Ref 5):

$$\left(\frac{\delta \ln \dot{\varepsilon}}{\delta \ln A}\right)_F = \frac{\gamma - 1}{m} \quad \text{(Eq 10)}$$

and

$$\frac{\delta \dot{A}}{\dot{A}} = \beta \frac{\delta A}{A} \quad \text{(Eq 11)}$$

The evolution of inhomogeneity due to mechanical damage can be calculated as:

$$\left(A_b\right)_{t+\Delta t} = \left(A_b\right)_t + \left(A_{t+\Delta t} - A_t\right)\left(\frac{A_b}{A}\right)^{\beta} \quad \text{(Eq 12)}$$

and

$$\dot{\varepsilon}_b = \dot{\varepsilon}\left(\frac{A_b}{A}\right)^{\frac{\gamma-1}{m}} \quad \text{(Eq 13)}$$

In order to study the instability and inhomogeneous deformation in a flow softening material, the constitutive equation of Jonas et al. (Ref 4) of the form given below was used:

$$\sigma = -A(-\dot{\varepsilon})^m[1-\exp(25\varepsilon)]\,(-\varepsilon)^{-0.375} \quad \text{(Eq 14)}$$

where $A(-\dot{\varepsilon})^m = 50$. Figure 1(a) shows this flow curve, along with a plot of $\partial\sigma/\partial\varepsilon$. The curves cross at two values of strain where Considere's criterion ($\sigma = \partial\sigma/\partial\varepsilon$) is satisfied. Figure 1(b) shows the plot of $\gamma$ as a function of strain. Considere's condition is satisfied at strains $\varepsilon_C$ and $\varepsilon_{C'}$ where $\gamma = 1$. Hart's condition is satisfied at two strains $\varepsilon_H$ and $\varepsilon_{H'}$ where $\gamma = (1 - m)$. The values of the Considere strains and the Hart strains for different strain-rate sensitivity values are listed in Table 1.

**Table 1 Considere and Hart strains for the constitutive equation used**

| Strain-rate sensitivity ($m$) | Considere strains | | Hart strains | |
|---|---|---|---|---|
| | $\varepsilon_C$ | $\varepsilon_{C'}$ | $\varepsilon_H$ | $\varepsilon_{H'}$ |
| | −0.0745 | −0.3643 | | |
| 0.1 | | | −0.07242 | −0.4064 |
| 0.3 | | | −0.06867 | −0.5257 |
| 0.6 | | | −0.06395 | −0.9275 |

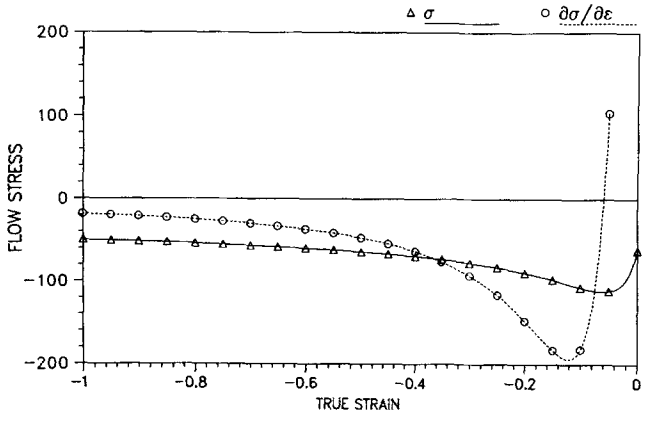


(a)

For the two cases studied using slab analysis, the starting cross sectional area of the specimen was assumed to be 100 units. In the case of the machining defect, a bulge of area 125 units was used. In the case of mechanical damage, the damaged region was assumed to have been prestrained to $\varepsilon_0 = -0.1$. The calculations were carried out for various values of $m$ to study the effect of strain-rate sensitivity. The prestrain was larger than the first Hart strain $\varepsilon_H$ for all values of strain-rate sensitivity used. These parameters are similar to those used in previous analyses (Ref 4).

## 3. FEM Simulation of Inhomogeneous Deformation During Compression

The slab method described above makes the simplified assumption that the disks of material deform independent of each other. Because this may not give an accurate picture of the deformation, FEM simulations of the same problems were carried out. The finite element program ALPID was used for this purpose. The constitutive equation used for this problem was:

$$\sigma = -B\left(-\frac{\dot{\varepsilon}}{\dot{\varepsilon}_0}\right)^m [1-\exp(25\varepsilon)]\,(-\varepsilon)^{-0.375} \quad \text{(Eq 15)}$$

where $\dot{\varepsilon}_0 = 0.1$ is the average strain rate. The value of $B$ was selected to maintain:

$$B\left(-\frac{\dot{\varepsilon}}{\dot{\varepsilon}_0}\right)^m = A(-\dot{\varepsilon})^m = 50 \quad \text{(Eq 16)}$$

for all values of strain-rate sensitivity, $m$. The deformation was assumed to occur isothermally, and all inhomogeneities de-

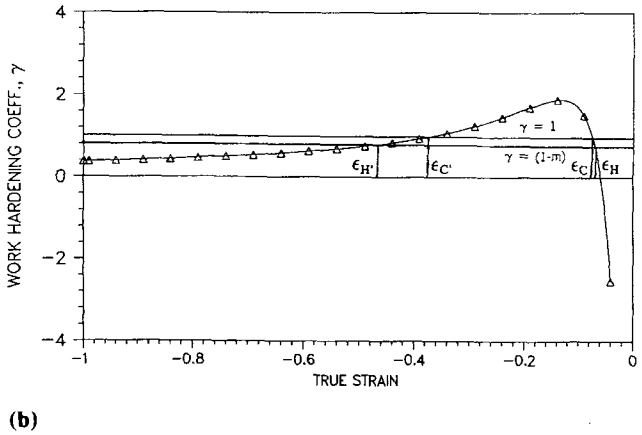


(b)

**Fig. 1** (a) Variation of flow stress, $\sigma$, and $(\partial\sigma/\partial\varepsilon)$ as a flow softening material. (b) Variation of $\gamma$ as a function of strain. At the Considere strains $\sigma = (\partial\sigma/\partial\varepsilon)$ and $\gamma = 1$, and at the Hart strains $\gamma = (1\text{-m})$.

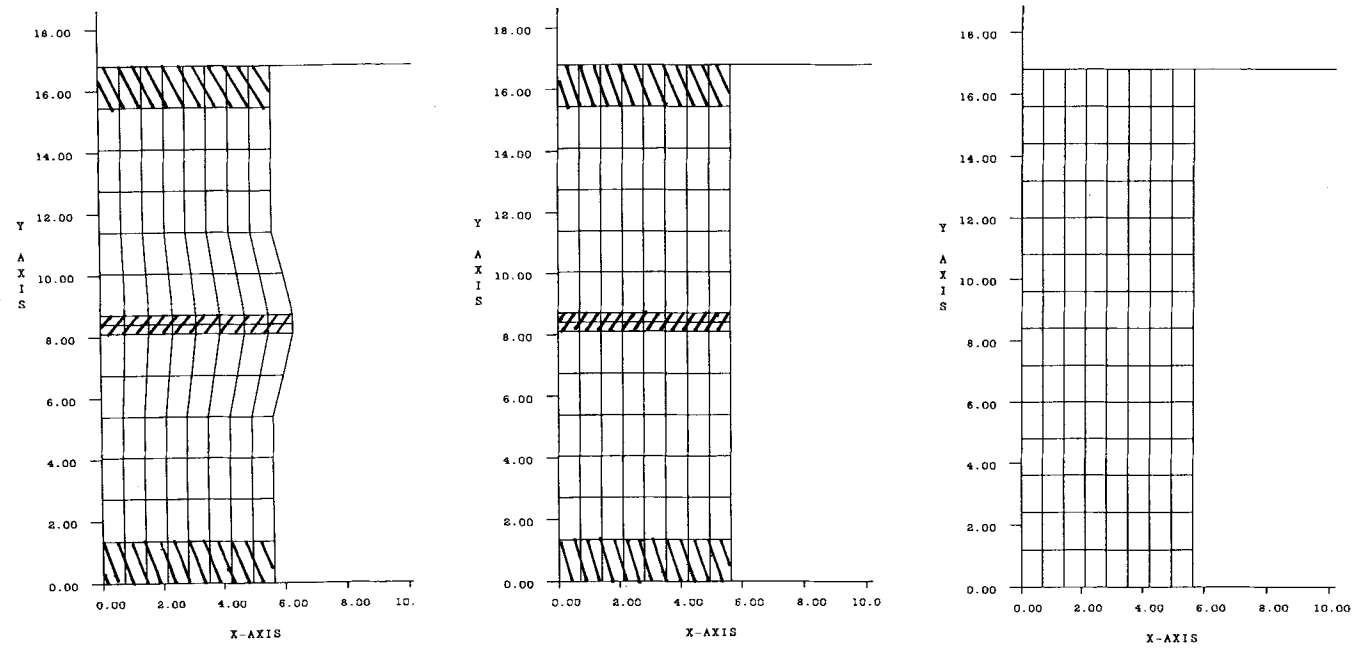


**Fig. 2** Starting FE mesh for three cases of inhomogeneous deformation. (a) Geometric inhomogeneity. (b) Mechanical damage. (c) Friction

velop due to the flow softening nature of the above constitutive equation. This is in contrast to the study by Oh, et al. (Ref 6), where flow localization occurs due to deformation heating and strain rate effects. Three cases of inhomogeneous deformation were considered: (1) a bulged cylinder (geometric variation or machining defect) deforming between frictionless platens, as discussed in the previous section, (2) a locally strained cylinder (mechanical damage) deforming without friction, and (3) a uniform cylinder with friction at the platen contact surfaces. In all cases, a cylinder of height 16.8 units was deformed by keeping the lower platen fixed and moving the upper platen down with an exponential displacement rate to maintain a constant strain rate of 0.1 units.

### 3.1 *Case 1: Effect of Machining Defect*

Figure 2(a) shows the starting mesh for this case. The deforming body is axisymmetric about the Y axis. An initial bulge was introduced by making a region at the middle of the body have a larger diameter. The area of cylindrical portion was 100 units while that at the bulge was 125 units, as used in the slab analysis above. The strain-rate sensitivity values used were $m$ = 0.1 and 0.6. In Fig. 2(a), the region of the bulge is identified by hatching with forward slashes, and the region in contact with the platens, representing the uniform region, is identified by two strips that are hatched with backward slashes.

### 3.2 *Case 2: Effect of Mechanical Damage*

In this case, the deforming body was assumed to be cylindrical, but a local region was given an initial prestrain to produce the effect of mechanical damage. Figure 2(b) shows the mesh used in this case. The mechanically damaged region is shown as two strips of 8 elements each at the center, indicated by hatching with forward slashes. The region hatched with backward slashes in contact with the top and bottom platens represents the undamaged region. The elements in the shaded region at the center were prestrained to $\bar{\varepsilon} = 0.1$. The strain-rate sensitivity values of $m = 0.1$ and 0.6 were assumed to represent typical values during hot forming and superplastic forming of metals, respectively.

### 3.3 *Case 3: Effect of Friction*

Friction between a workpiece and a die is unavoidable during metal forming and sometimes leads to nonhomogeneous deformation and the formation of shear bands, especially during the hot forging of a flow softening material (Ref 7). The mesh for this case is shown in Fig. 2(c). A constant shear friction factor of 0.2 was assumed between the cylinder and the platens. Strain-rate sensitivity values of $m$ = 0.1, 0.3, and 0.6 were considered to cover a wide range of $m$.

## 4. Results and Discussions

### 4.1 *Slab Analysis of Inhomogeneity in Compression*

#### 4.1.1 Effect of a Machining Defect

Figure 3(a) shows the change in the areas of the bulge and uniform regions for different values of strain-rate sensitivity $m$. Figure 3(b) shows the change in the strain rate, and Fig. 3(c)

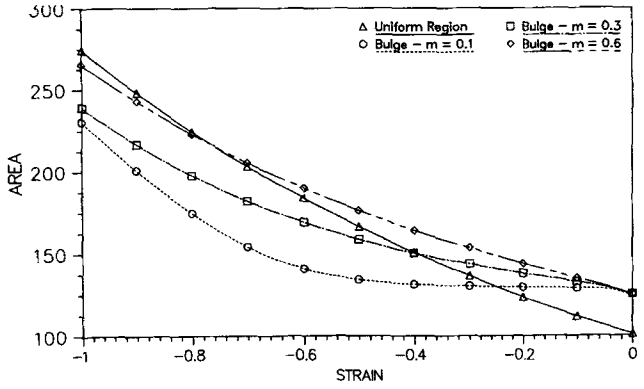


(a)

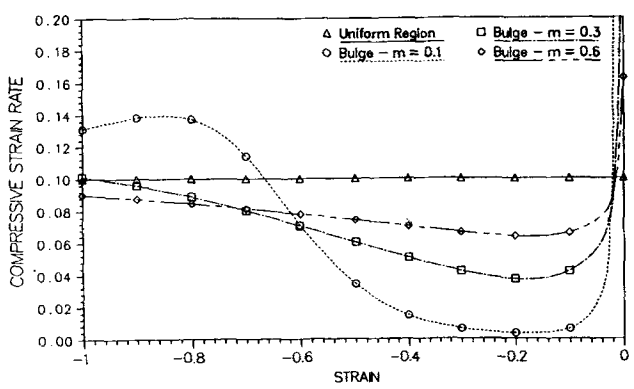


(b)

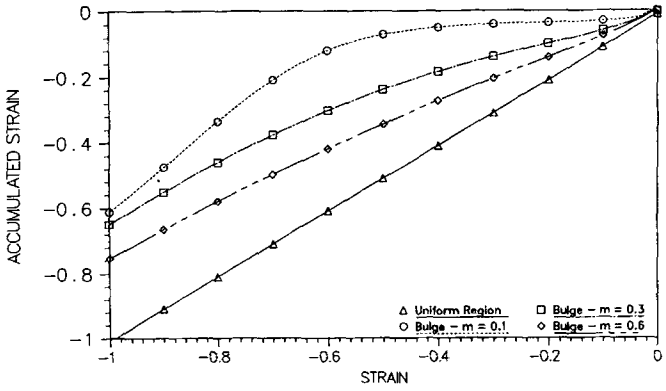


(c)

**Fig. 3** Effect of strain-rate sensitivity, $m$, on the variation of (a) the area, (b) the strain rate, and (c) the accumulated strain in the bulge

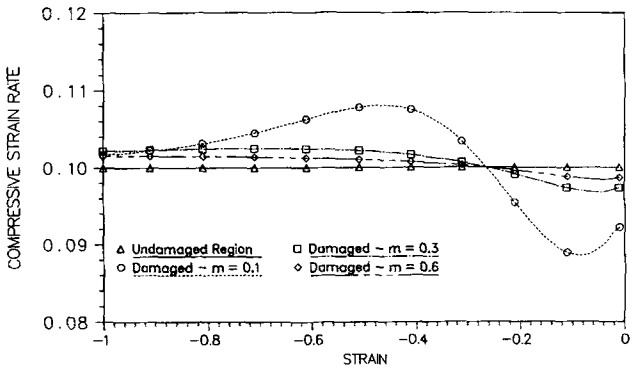


(a)

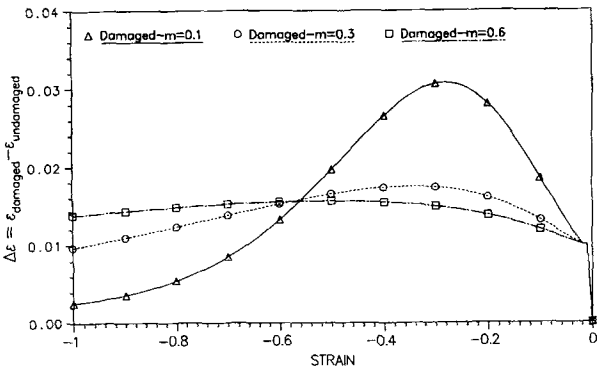


(b)

**Fig. 4** Effect of strain-rate sensitivity, $m$, on (a) the strain rate in the damaged region and (b) the difference between the accumulated strain in the damaged region and that in the undamaged region.

shows the accumulated strain in the bulge and uniform regions of a bulged cylinder undergoing compression. The initial difference in area between the uniform and bulged sections was 25 units (25%). In Fig. 3(a), the area of the uniform region increases exponentially with strain, i.e., $A = A_0 \exp(-\varepsilon)$. The bulge region initially deforms for all values of $m$. For a low strain-rate sensitivity ($m = 0.1$), the bulge, being of larger area, essentially stops deforming, i.e., the strain rate is almost nil (Fig. 3b). On the other hand, the uniform region continues to deform, and its area increases, exceeding that of the bulge beyond a strain of approximately –0.26. When the area of the uniform region has increased sufficiently, the bulge starts to deform again. After a strain of approximately –0.66, the region of the bulge deforms with a higher strain rate than the uniform region (Fig. 3b), and its area increases faster than that of the uniform region (Fig. 3a). As seen in Fig. 3(c), the accumulated

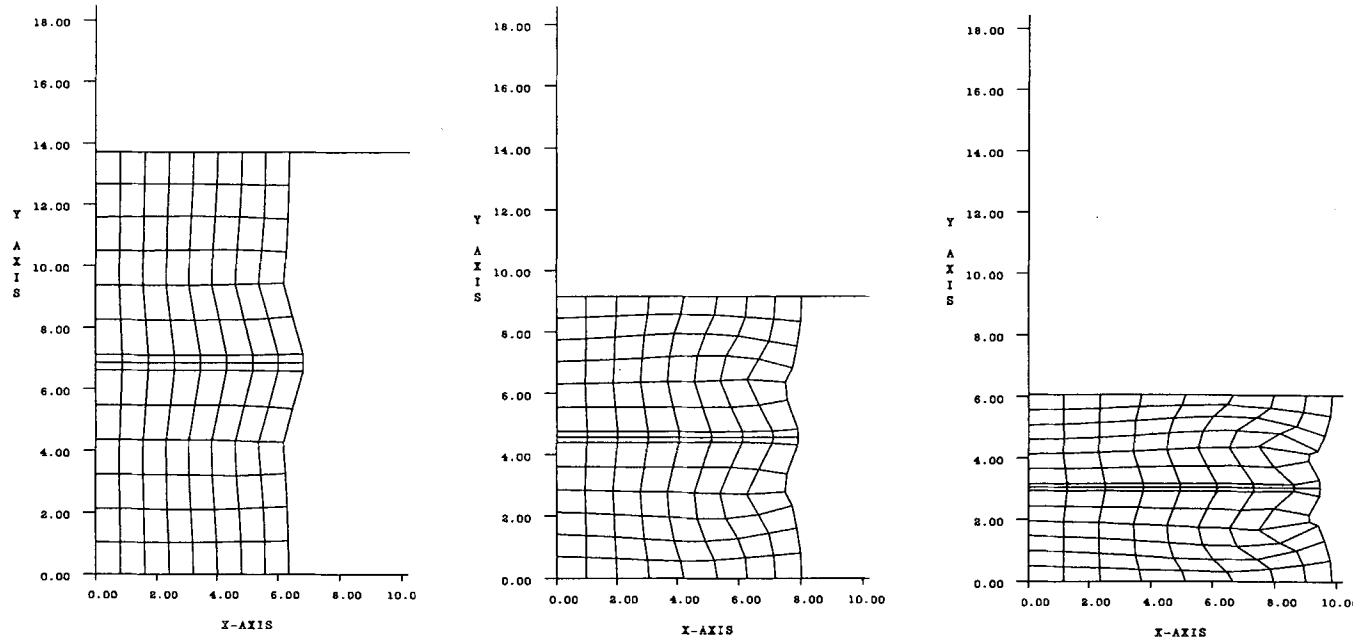


**Fig. 5** Finite element meshes showing the evolution of a geometric inhomogeneity for strain-rate sensitivity $m = 0.1$. (a) $\varepsilon = -0.2$ (b) $\varepsilon = -0.6$ (c) $\varepsilon = -1.0$

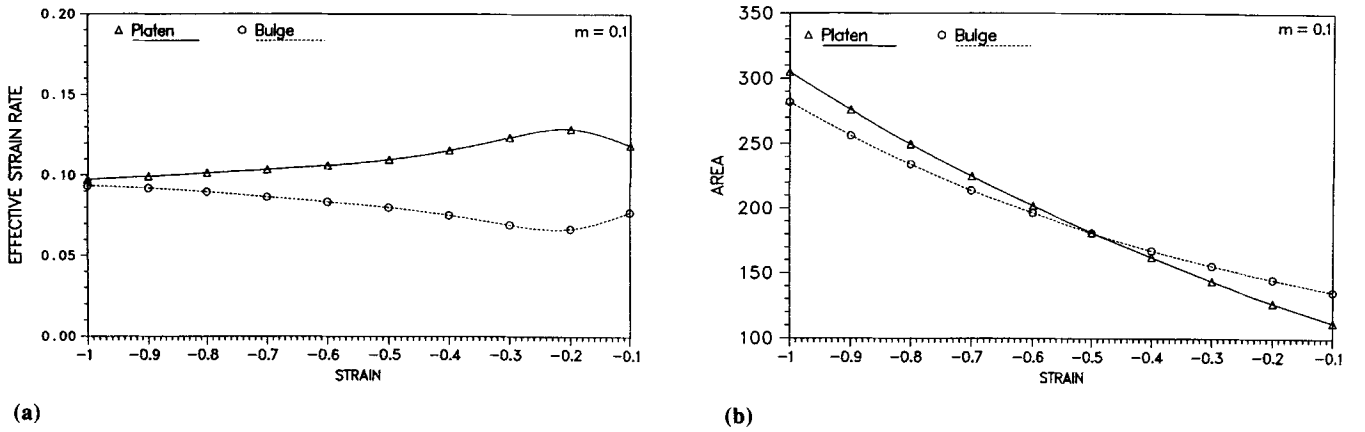


**Fig. 6** (a) Variation with strain of the average strain rate in the regions in contact with the platens and that in the region of the bulge when strain-rate sensitivity $m = 0.1$. (b) Variation with strain of the area in contact with the platens and the area of the bulge.

strain in the bulge region is less than that in the uniform region up to a strain of –1. Because the material flow softens, the bulge region is harder than the uniform region. Therefore, after further deformation to a strain of approximately –0.84, the strain rate in the bulge begins to decrease. Thus at a low strain-rate sensitivity, the strain-rate in the bulge oscillates.

At higher values of $m$, the strain rate in the bulge quickly decreases to less than that in the uniform section, but does not go to zero. The bulge and uniform sections deform continuously, and the strain rate in the bulge approaches that in the uniform section at large strain. Figure 3(c) shows that with increasing $m$, the accumulated strain in the bulge gets closer to that in the uniform region. The deformation is therefore more uniform at higher values of strain-rate sensitivity $m$.

### 4.1.2 Effect of Mechanical Damage

The prestrain due to the mechanical damage is greater than the strain at peak stress. The damaged region is, however, initially harder than the undamaged region. Therefore, as seen in Fig. 4(a), the damaged region deforms slower than the bulk. However, after the strain in the damaged region reaches the second Considere strain, strain rate localization occurs in the damaged region of all values of strain-rate sensitivity. But, the

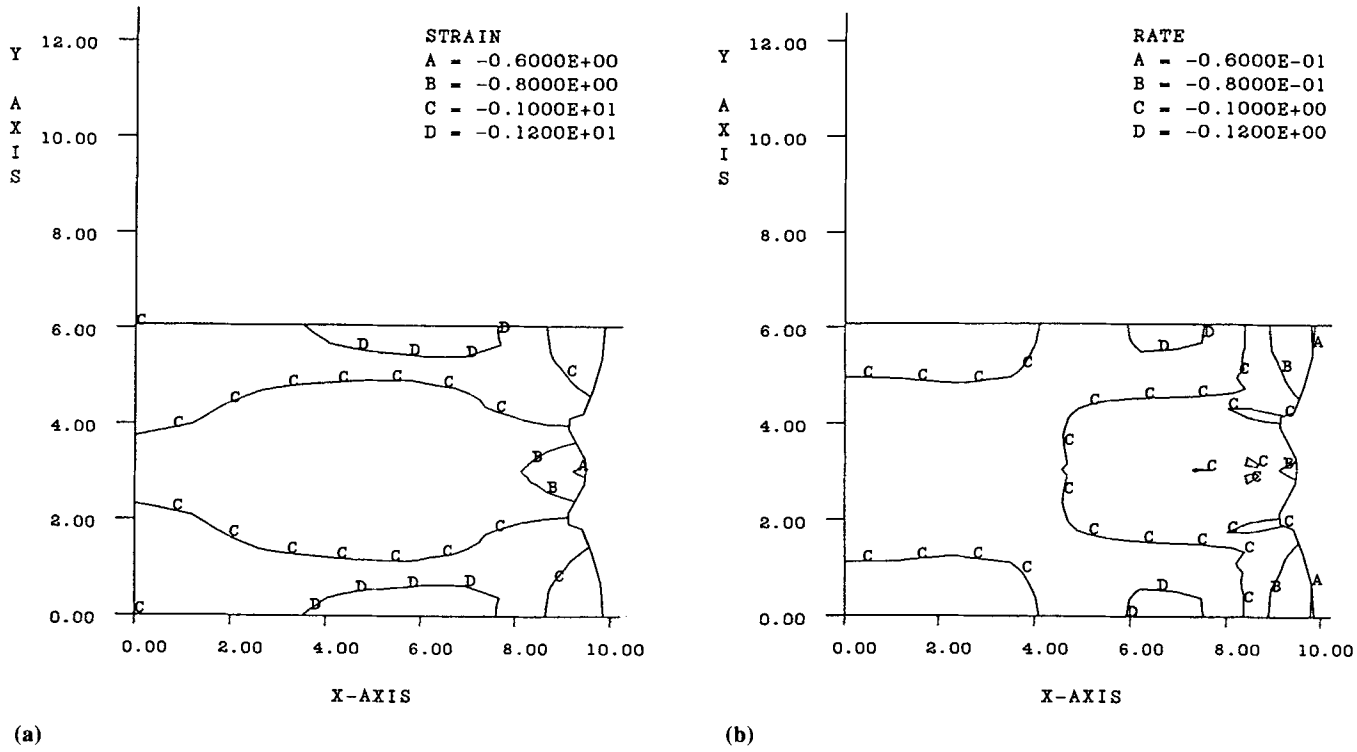


**Fig. 7** Predicted contours of (a) strain and (b) strain rate in the deformed sample when nominal strain = −1.0 and strain-rate sensitivity $m = 0.1$

deviations of strain rate in the damaged region from that in the undamaged region decrease as $m$ increases.

The damaged and undamaged regions initially have the same area. Figure 4(b) shows the difference between the strains in the two regions accumulated during the deformation. At a strain-rate sensitivity $m = 0.1$, when the strain rate is initially higher in the undamaged region (Fig. 4a), a strain difference of ~0.03 develops (Fig. 4b). At higher strain-rate sensitivities, the greatest difference in accumulated strain is less, but persists for a longer duration of strain. However, the difference in the total accumulated strain, $\Delta\varepsilon$, is quite low (<0.035), and no significant flow localization occurs.

The results of slab analysis clearly show that deformation is more homogeneous, i.e., the strain and strain rate difference between the bulk and defect region are less when the strain rate sensitivity is high. However, for the parameters used, the development of inhomogeneous deformation during compression of a flow softening material is apparently unrelated to the Hart strains.

## 4.2 *FEM Analysis of Inhomogeneity in Compression*

### 4.2.1 Effect of Machining Defect

Figure 5 shows the FE mesh at three different strains when $m = 0.1$. The regions near the platens have a smaller area and, therefore, deform faster than the bulge. The less strained and therefore stronger bulge restrains the deformation of regions just above and below it. The accumulated strain near the top and bottom makes these regions softer, facilitating further deformation. These factors lead to the development of grooves just above and below the original bulge (Fig. 5c).

Figure 6(a) shows the average strain rate in the sixteen elements comprising the central part of the bulge and that in the sixteen elements in contact with the platens. Figure 6(b) shows the area in contact with the platens and the area of the bulge calculated based on the radial coordinate of the outermost node. The bulge deforms at a slower strain rate than do the platen regions. The difference in strain rate increases up to a strain of 0.2 and then decreases. As a result, the area of the platen regions becomes greater than that of the bulge at a strain greater than 0.5. Though the average strain rates in the two regions approach the imposed nominal strain rate of 0.1 at higher strains, the strain rate is nonuniform, and the total deformation is inhomogeneous at a total strain of −1.0, as indicated in Fig. 7.

Figure 8 and 9 show the FE mesh and the areas and the average strain rates when $m$ is assumed to be 0.6. When these figures are compared to the corresponding figures for $m = 0.1$, a different pattern of deformation can be seen. The average strain rates in the platen and bulge regions remain almost constant and are only slightly different from the imposed strain rate (Fig. 9a). The areas of all regions change exponentially with imposed strain, and a severe notch does not develop (Fig. 8 and 9b). Though the bulge is preserved, there are smaller variations in strain, and strain rate contours in Fig. 10(a) and (b) indicate that the deformation is substantially homogeneous.

Figure 11(a) shows the change in $\Delta A$ ($= A_{bulge} - A_{platen}$) as a function of strain-rate sensitivity at different strains. $\Delta A$ is initially positive and decreases with increasing compressive strain when $m$ is small. When $m = 0.1$, $A_{platen}$ becomes larger than $A_{bulge}$ after a strain of approximately −0.5. For values of $m$

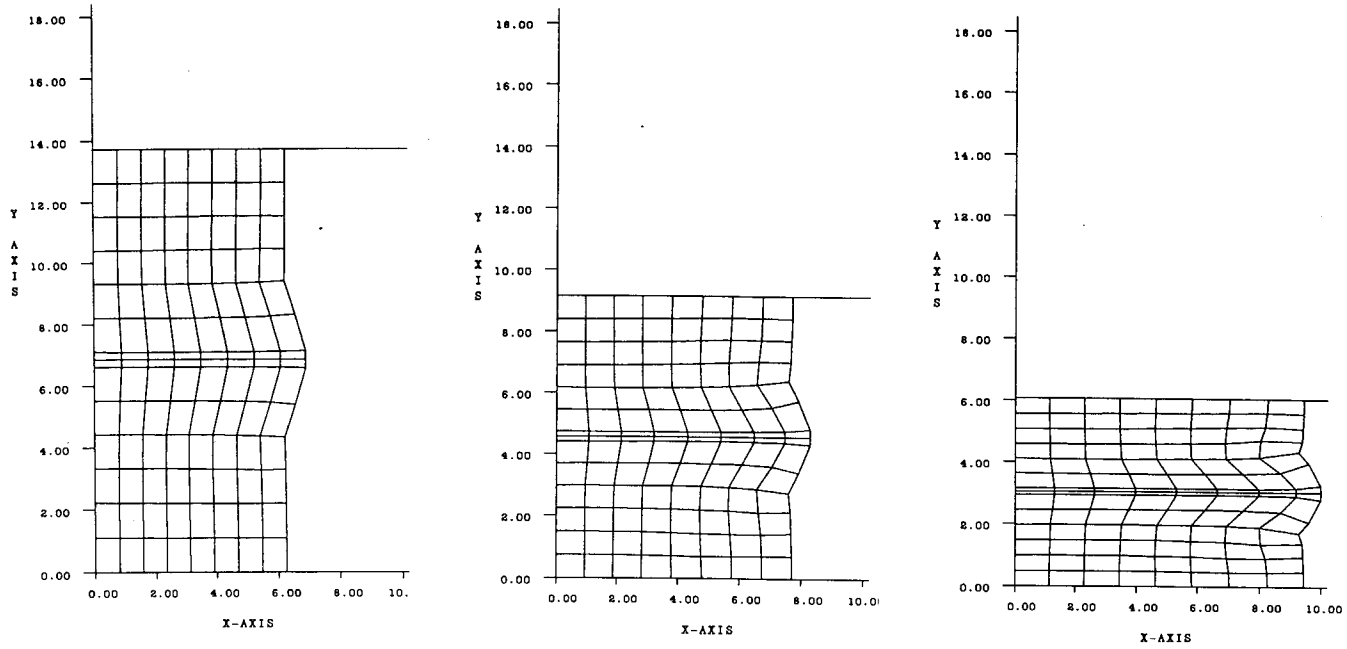


(a) (b) (c)

**Fig. 8** Finite element meshes showing the evolution of a geometric inhomogeneity for strain-rate sensitivity $m = 0.6$. (a) $\varepsilon = -0.2$ (b) $\varepsilon = -0.6$ (c) $\varepsilon = -1.0$

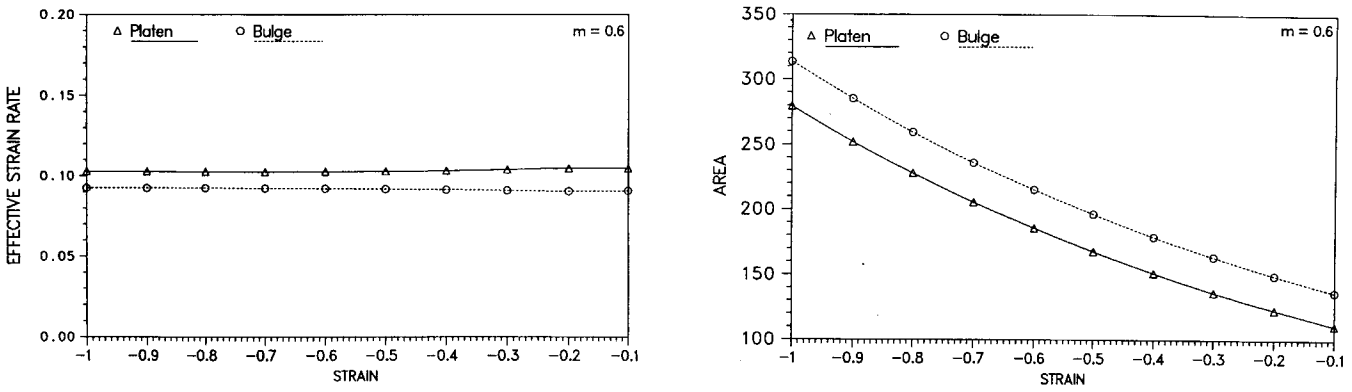


(a) (b)

**Fig. 9** (a) Variation with strain of the average strain rate in the regions in contact with the platens and that in the region of the bulge when strain-rate sensitivity $m = 0.6$. (b) Variation with strain of the area in contact with the platens and the area of the bulge.

greater than ~0.4, $\Delta A$ increases with strain. For a value of $m = 0.38$, the initial value of $\Delta A = 25$ is maintained up to a strain of 1, as shown in Fig. 11(b).

Practical implications of these results are that if a material has a high strain-rate sensitivity, all regions of a body with nonuniform cross section deform at fairly uniform deformation rates. Such a material can, therefore, be deformed to large strains without localization, i.e., the material is superplastic. Because deformation gets distributed, intricate shapes can be formed with superplastic materials.

### 4.2.2 Effect of Mechanical Damage

Figures 12(a) and (b) show the evolution of area and strain rate when $m = 0.1$. The prestrain of 0.1 puts the damaged region in the flow softening part of the stress-strain curve. At this strain level, the damaged region is initially harder than the undamaged region and deforms at a slower rate. However, after a nominal strain of –0.04, the damaged region deforms at a considerably greater strain rate than the undamaged region deforms. This is because the total strain (prestrain + accumulated strain) in the damaged region is larger than that in the undamaged region, which makes the damaged region softer. This results in the development of a bulge as shown in Fig. 13(a). Because the area in the bulge is now greater than that of the undamaged region, the strain rate in the bulge decreases and becomes less than that in the undamaged region at strains more than approximately –0.7. The bulge, however, persists to a strain of –1.0. The strain contours for the case of $m = 0.1$ in Fig.

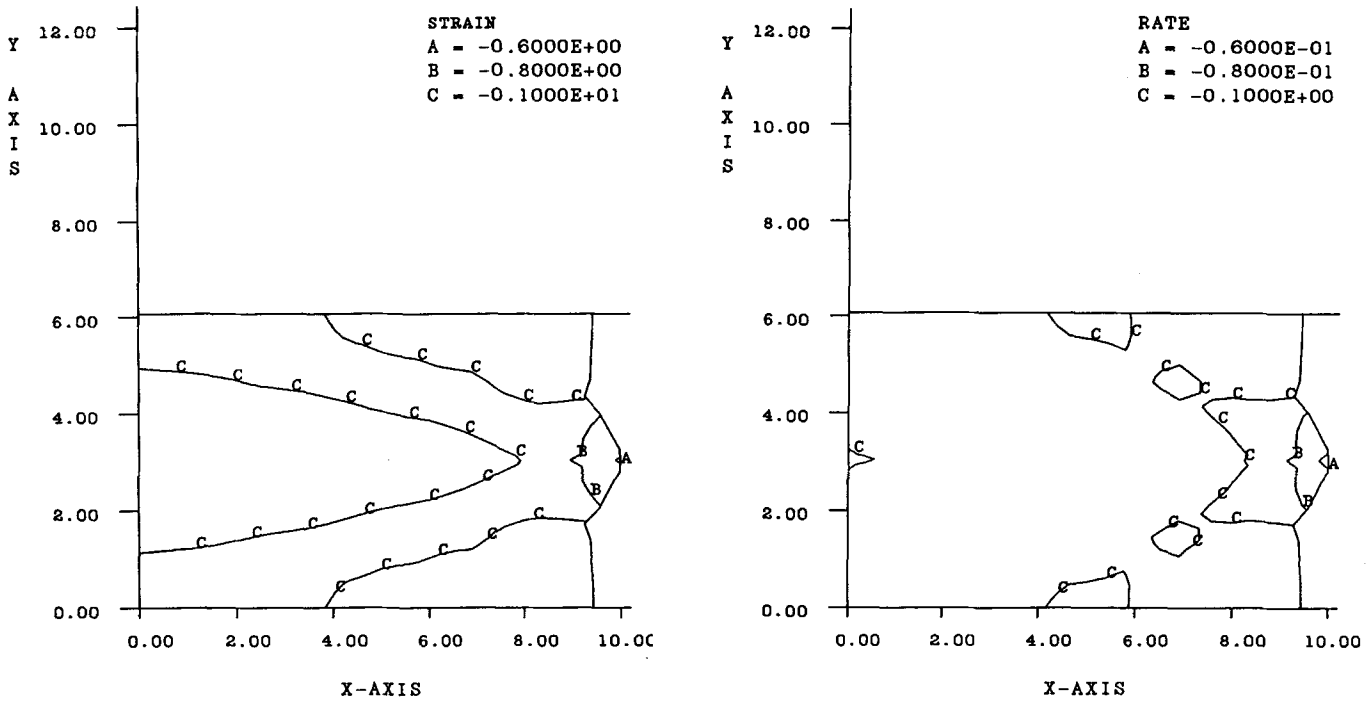


(a) (b)

**Fig. 10** Predicted contours of (a) strain and (b) strain rate in the deformed sample when nominal strain = –1.0 and strain-rate sensitivity $m = 0.6$.

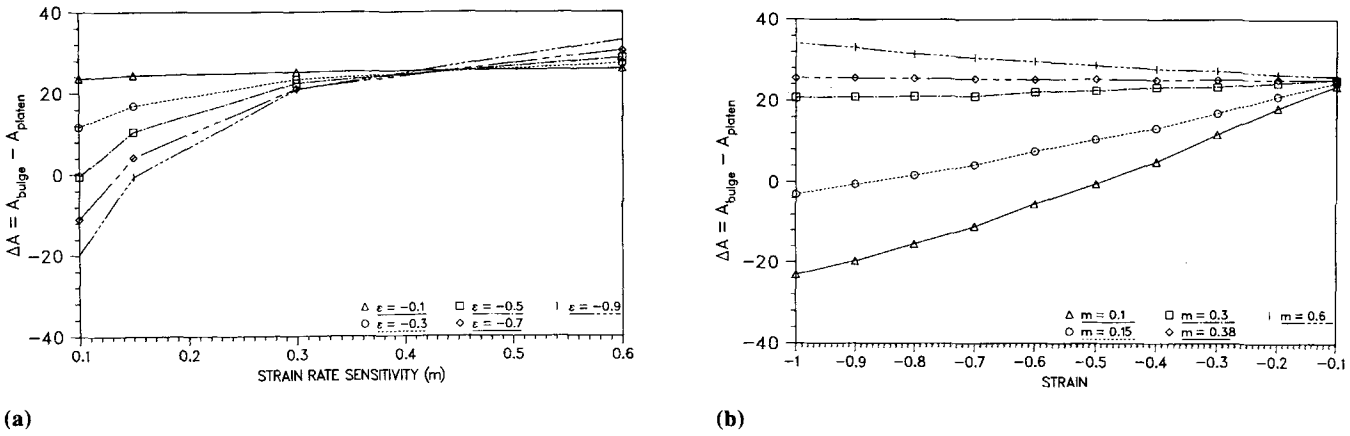


(a) (b)

**Fig. 11** (a) Change in $\Delta A$, the difference between the area of the bulge and the area in contact with the platen, as a function of strain-rate sensitivity, $m$, at different strains. (b) Effect of strain-rate sensitivity, $m$, on the evolution of $\Delta A$.

13(b) show that indeed the deformation is localized in the damaged region. Further, the strain rate contours in Fig. 13(c) also show that the overall deformation is nonhomogeneous, as there is a significant variation in strain rate within the sample.

When the strain-rate sensitivity is increased to 0.6, again the deformation rate in the damaged region is initially less than in the undamaged region, and there is a cross over at a strain of approximately –0.04. But the strain rates in the damaged and undamaged regions differ by only a small amount (Fig. 14b). At strains beyond –0.6, the strain rates in the two regions remain approximately the same as the imposed average strain rate. The difference in area between the damaged and undamaged regions is considerably less than when $m = 0.1$ (Fig. 12a and 14a). Figure 15(a) shows the deformed FE mesh after a strain of 1.0. The strain and strain rate contours in Fig. 15(b) and (c), respectively, again show that the deformation is more homogeneous when compared to the case of $m = 0.1$.

### 4.2.3 Effect of Friction

Friction is probably a far more important parameter during metal forming than a large variation in initial area and a severe mechanical damage, such as the large bulge and the prestrain of

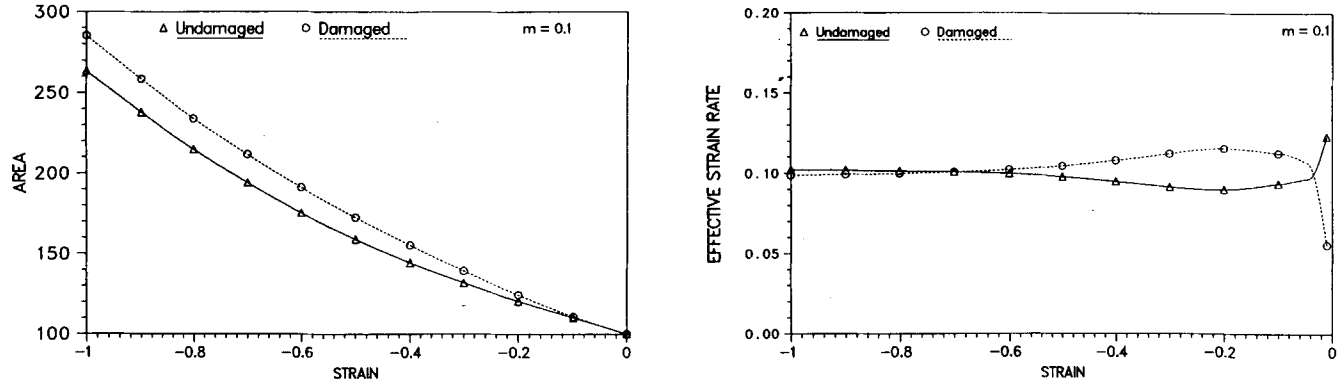


**Fig. 12** (a) Evolution of the areas of the undamaged and the damaged regions when strain-rate sensitivity $m = 0.1$. (b) Change in the average strain rate in the damaged and undamaged regions as a function of strain.

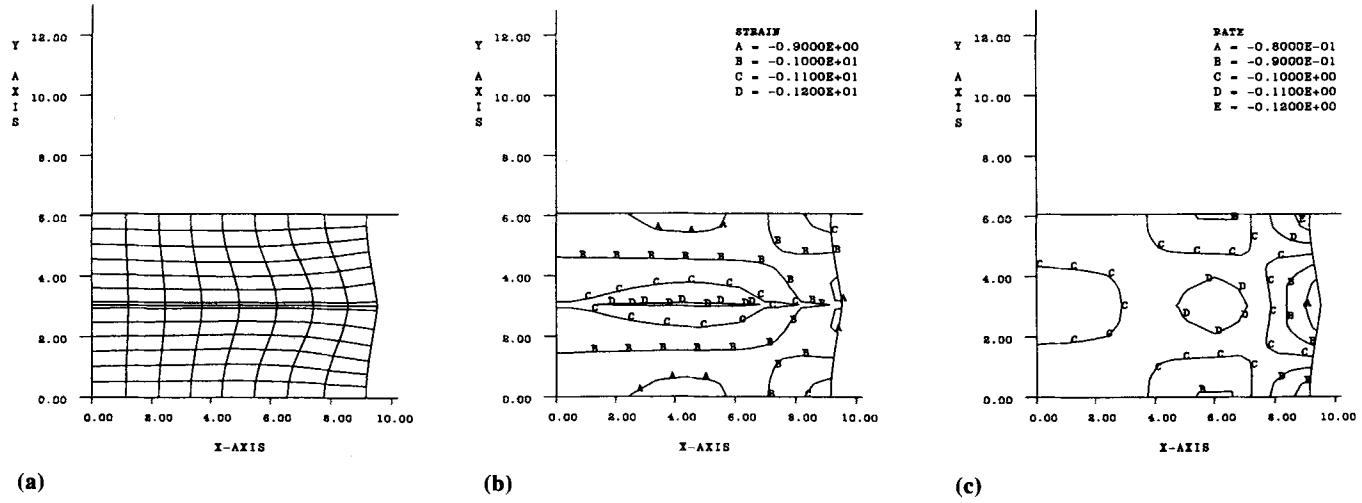


**Fig. 13** Deformed FE mesh, (b) Predicted strain contours, and (c) predicted strain rate contours after deformation to a strain of −1.0 when strain-rate sensitivity $m = 0.1$.

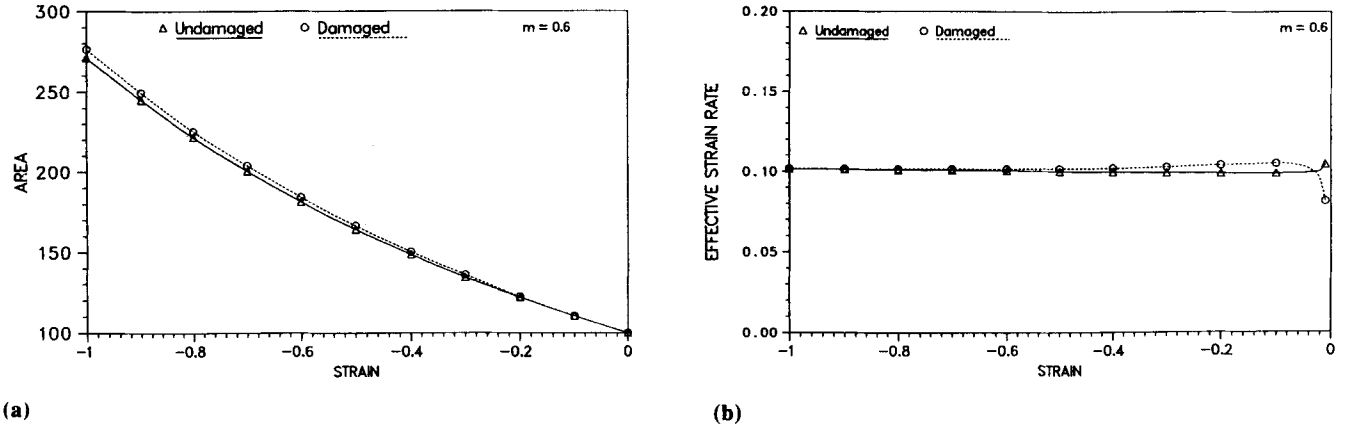


**Fig. 14** (a) Evolution of the areas of the undamaged and the damaged regions when strain-rate sensitivity $m = 0.6$. (b) Change in the average strain rate in the damaged and undamaged regions as a function of strain.

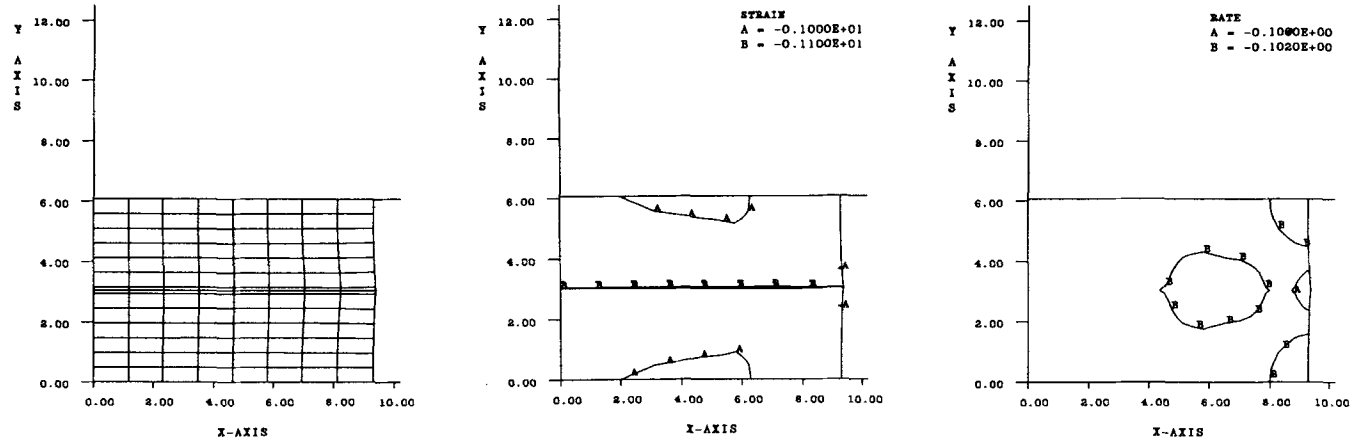


**Fig. 15** (a) Deformed FE mesh, (b) predicted strain contours, and (c) predicted strain rate contours after deformation to a strain of −1.0 when strain-rate sensitivity $m = 0.6$.

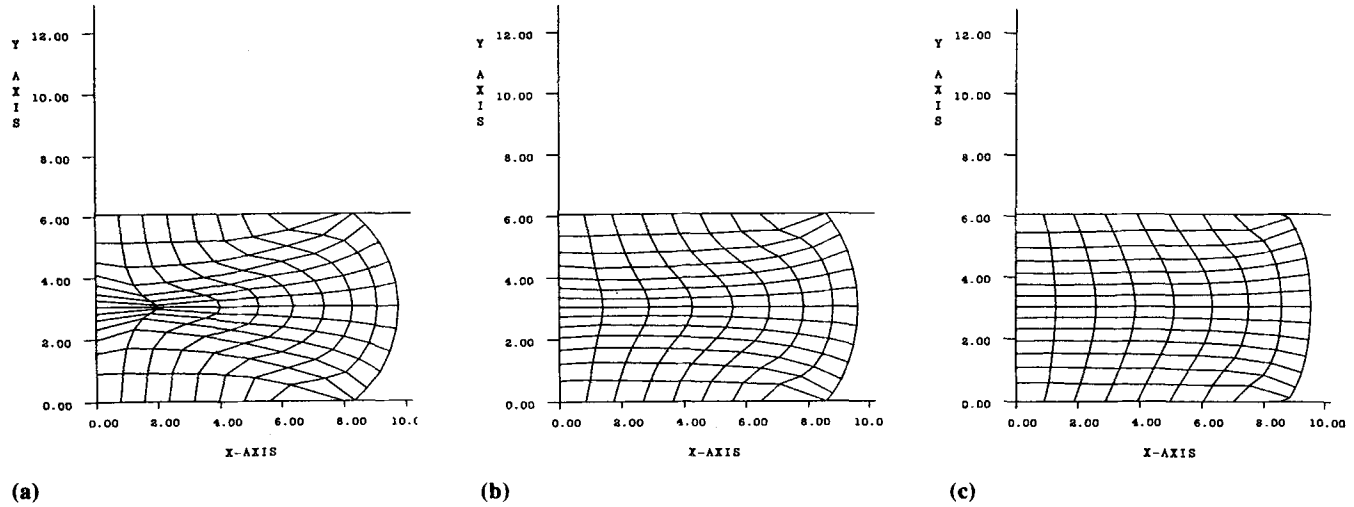


**Fig. 16** Deformed FE meshes for the case of friction between the platen and sample showing the effect of strain-rate sensitivity. (a) $m = 0.1$ (b) $m = 0.3$ (c) $m = 0.6$

0.1 considered above. For this part of the study, a constant shear friction factor of 0.2 was assumed. Figures 16(a), (b), and (c) show the deformed grid at a strain of −1.0 for three values of $m = 0.1$, 0.3, and 0.6, respectively. The formation of a shear band at the low strain rate sensitivity of $m = 0.1$, as indicated by severely distorted elements, is evident. The strain contour plot in Fig. 17(a) shows that for a small value of $m$, a large gradient of strain develops across the shear band, and there is a dead metal zone that has undergone little deformation. These effects decrease for higher values of $m$ (Fig. 17b and c). The strain rate contour plots in Fig. 18 also show a similar effect with higher strain rates concentrated in the region of shear band for low value of $m = 0.1$ (Fig. 18a). For a value of $m = 0.6$, the strain rates are uniform across most of the sample, and the shear band is not formed (Fig. 18c).

To follow the development of inhomogeneity in deformation in this case, where friction is the primary cause, the variance in the strain rate among all the elements was calculated as $\Sigma(\dot{\varepsilon}_i - \dot{\varepsilon}_{avg})^2$ at each strain. Due to the friction, a variation in strain rate exists for all values of $m$. But in all cases, the average strain rate was found to be equal to the imposed strain rate of 0.1. For a low value of $m = 0.1$, a large variation in strain rate develops, reaching a maximum value of ~0.0027 at a strain of −0.53, as shown in Fig. 19. As $m$ is increased, the maximum variation in strain rate decreases. However, $m$ does not seem to have a significant effect on the period over which large strain rate variations occur.

## 5. Summary and Conclusions

This paper includes results of a parametric study on the development of inhomogeneities during compressive deformation of a flow softening material. Both finite element analysis

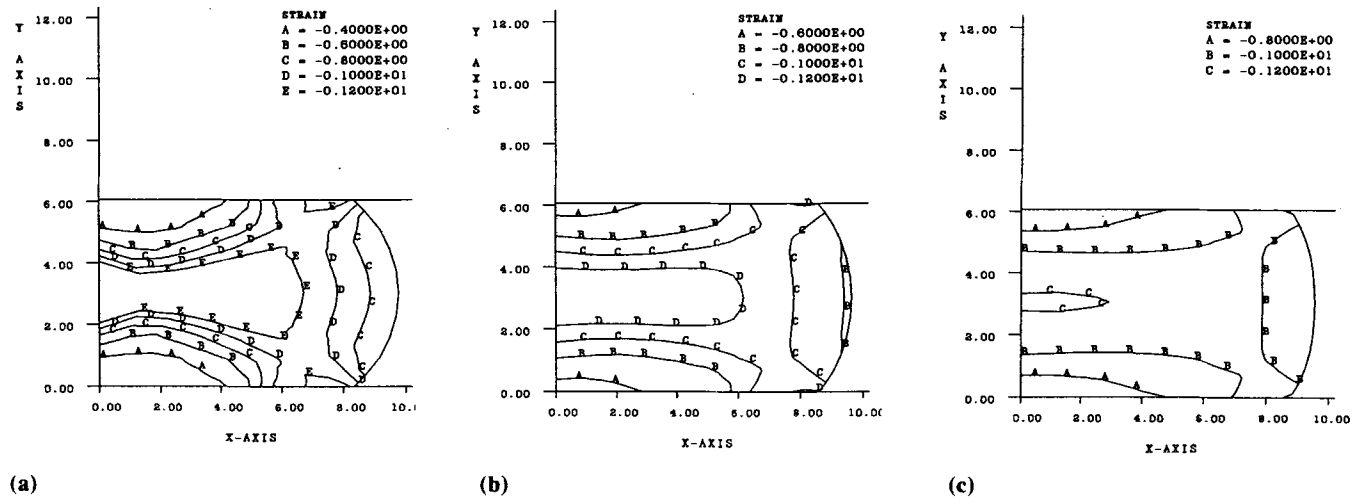


**Fig. 17** Predicted strain contours for the case of friction between the platen and sample for different values of strain-rate sensitivity. (a) $m = 0.1$ (b) $m = 0.3$ (c) $m = 0.6$

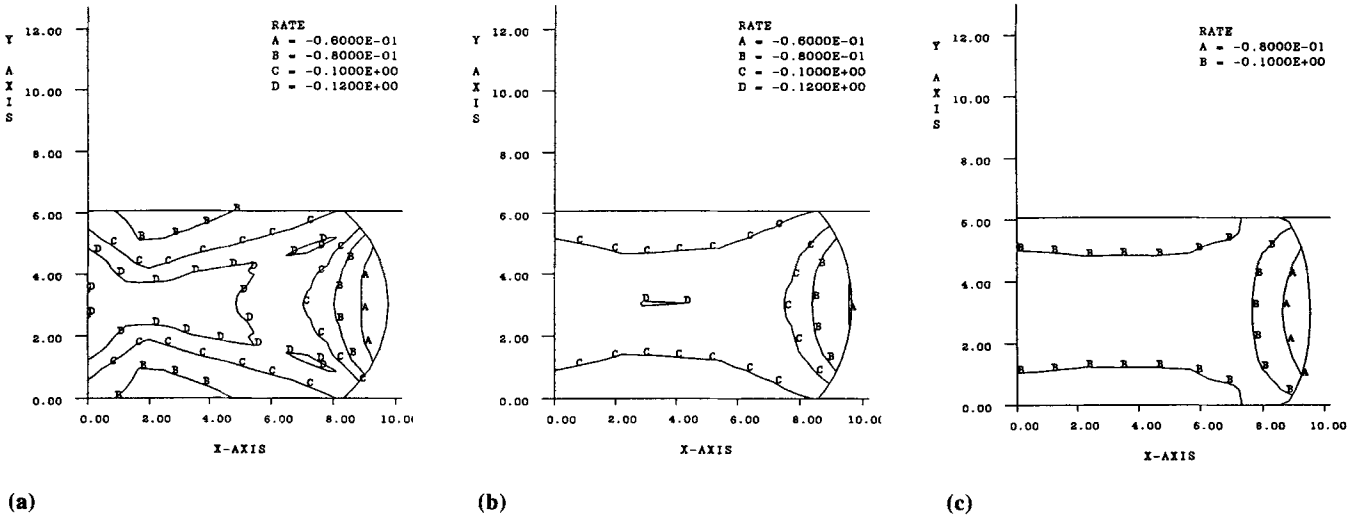


**Fig. 18** Predicted strain rate contours for the case of friction between the platen and sample for different values of strain-rate sensitivity. (a) $m = 0.1$ (b) $m = 0.3$ (c) $m = 0.6$

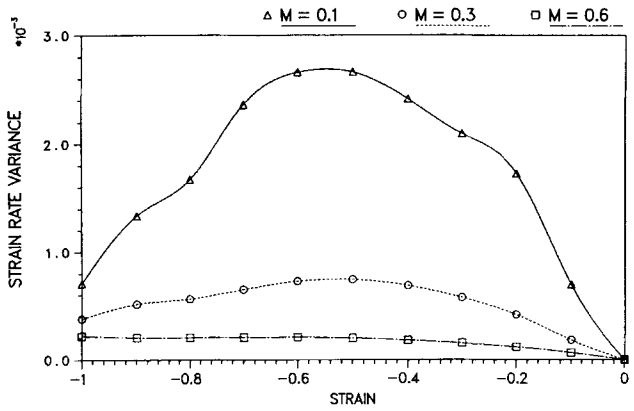


**Fig. 19** Effect of strain-rate sensitivity, $m$, on the predicted variance in strain rate within a sample during compressive deformation

and the slab method show that as strain-rate sensitivity increases deformation is more uniform. However, the analyses did not show any correlation between the occurrence of flow localization to the two Hart strains.

In the case of a machining defect (bulge), both the slab method and FEM predict that the bulge initially deforms at a slower strain rate than the bulk. Slab analysis results show that at low values of $m$, the bulge may deform at a faster strain rate than the bulk after a critical strain. FEM, on the other hand, predicts that the bulge will always deform at a slower strain rate than the bulk, but the differences decrease with increasing $m$. Slab analysis predicts that the area of the uniform part of the sample will exceed that of the (initial) bulge after some deformation. However, FEM predicts that this will happen only at low $m$ values.

Both the FEM and the slab method show that if a part of the compression specimen is prestrained due to mechanical damage, then deformation inhomogeneities can develop. Again, the extent of inhomogeneous deformation decreases as the strain-rate sensitivity is increased. The slab method, however, shows that greater amounts of strain rate localization than that predicted by the FEM can occur.

Under isothermal forming conditions, friction plays a significant role in causing deformation inhomogeneities, which appear in the form of dead metal zones and shear bands. FE analysis shows that as the strain-rate sensitivity increases, more uniform deformation occurs, as indicated by a smaller dead metal zone, absence of shear bands, and less barreling.

## Acknowledgment

This symposium paper was presented at the TMS Annual Meeting, Denver, CO, February 21-25, 1993 and published in *Computer Applications in Shaping and Forming of Materials*, Mahmoud Y. Demeri, Ed., TMS, Warrendale, PA, 1993. Support from the Air Force Office of Scientific Research through grant No. AFOSR-90-0204, Dr. Alan H. Rosenstein, Program Manager, is gratefully acknowledged.

## References

1. J.J. Jonas and M.J. Luton, *Advances in Deformation Processing*, Plenum Publishing Corporation, 1978, p 215-233
2. A. Considere, *Ann. des Ponts & Chaussees*, Vol 9 (No. 6), 1885, p 574
3. E.W. Hart, *Acta Metall.*, Vol 15, 1967, p 351-355
4. J.J. Jonas, R.A. Holt, and C.E. Coleman, *Acta Metall.*, Vol 24, 1976, p 911-918
5. J.J. Jonas and B. Baudelet, *Acta Metall.*, Vol 25, 1977, p 43-50
6. S.I. Oh, S.L. Semiatin, and J.J. Jonas, *Metall. Trans. A*, Vol 23, 1992, p 963-975
7. S.L. Semiatin and G.D. Lahoti, *Metall. Trans. A*, Vol 13, 1982, p 275-288